NASA DEVELOP National Program
Pop-Up Project

Spring 2024

Intermountain West Wildland Fires

Mapping Tree Mortality and Burn Patches using NASA Earth Observations to Determine Fire Risk and Inform Fire Management Practices

DEVELOP Technical Report
March 29th, 2024

Teo Rautu (Project Lead)
Mark Cervantes
Britt Hays
Alec Wallen

Advisors:
Dr. Di Yang, University of Wyoming (Science Advisor)
Dr. Austin Madson, University of Wyoming (Science Advisor)

Lead:
Truman Anarella (Colorado – Fort Collins)

1. Abstract

Within the intermountain west, monitoring vegetation fuel loads is a major component of wildland fire management efforts. To address this concern, we partnered with the U.S. Forest Service to inform the agency which forested areas should be prioritized for prescribed burning and fuel reduction near human communities in the Bridger-Teton National Forest, Wyoming. We computed burn severity maps, fuel load maps, and a tutorial document to identify forest impact trends and provide the partner with the tools to replicate project methods for use in other wildfire crisis strategy sites. These end products were made using two NASA Earth observations: Landsat 8 Operational Land Imager and Shuttle Radar Topography Mission. Based on our random forest analysis, our maps identified 998 acres within the Wildland Urban Interface that are predicted to have high fuel loading and high burn severity within the Bridger-Teton National Forest. Forested areas closer to heavily populated areas such as Jackson, Kelly, Moran, New Forks Lake, and Star Valley Ranch should be prioritized for fuel reduction. However, our random forest model analysis was limited to using vegetation and topographical indices with no field data for model validation. Therefore, future studies should use field data for model validation to improve model accuracy and additionally incorporate Global Ecosystem Dynamics Investigation data into models to create better predictions of forested areas with high fuel load and high burn severity.

Key Terms

Remote Sensing, Landsat, Fuel Loads, Burn Severity, Wildland Urban Interface, Bridger-Teton National Forest

2. Introduction

2.1 Background Information

As current climatic conditions in the Rocky Mountains continue to warm (Shukla et al., 2022), there is an increased probability of unprecedented fire cycles extending beyond the historic fire range of the last millennia (Clark-Wolf et al., 2023). Higher severity fires increase rates of vegetation mortality and total area burned, threatening not only wildlife habitat, hydrological processes, and ecosystem services (Morton et al., 2003) but also human communities in wildland urban interfaces (WUI; Radeloff et al., 2005). Since the 1990s, the number of homes within wildfire perimeters has doubled in the conterminous United States (Radeloff et al., 2023). As urban development grows and expands, more structures are at risk of burning in WUIs, defined as "the line, area, or zone where structures and other human development meet or intermingle with undeveloped wildland or vegetative fuels" (Department of Agriculture & Department of Interior, 2001).

According to Radeloff et al. (2023), more than 60% of houses in Wyoming exist within a WUI. Yet, homes surrounded by rangeland and undeveloped land face increased wildland fire threats bolstered by high fuel loads. While it is increasingly critical for federal agencies such as the U.S. Forest Service (USFS) to determine which rangeland high fuel load areas to focus on for fuel reduction and crisis planning efforts. Tools that remotely sense wildland fires, vegetation conditions, and fuel density can improve forest management decisions, giving land managers an opportunity to reduce the impacts of fire (Hoffrén et al., 2023, Stefanidou et al., 2020; Furniss et al., 2020; Scott et al., 2013). One of the national forests that the USFS is interested in applying remote sensing tools for fuel reduction is the Bridger-Teton National Forest (BTNF; Figure 1) due to its potential for management comparison to other national forests within USFS Region 4 (a.k.a. Intermountain Region). The BTNF encompasses 3.4 million acres of undeveloped land with 13 or more WUIs, buttresses two national parks, and comprises three dedicated wilderness areas, creating one of the largest contiguous wilderness zones in the United States (U.S. Department of Agriculture, n.d.). The most common forested vegetation cover types found within the BTNF is subalpine fir, Engelmann spruce, and Douglas-fir forests which comprises 21% of the area (LANDFIRE, 2016). Forested areas are conducive to larger fuel loads and fuel bed bulk density that drive landscape-fire connectivity (Miller and Urban 2000, Deeming et al., 1972). Scott et al. (2012) simulated the likelihood of prescribed fires in the BTNF reaching Jackson, Wyoming under "let it burn" or active suppression conditions. Simulated fires managed with prescribed burns resulted in less severe, smaller, and shorter duration fires that were less likely to reach WUI areas in comparison to unmanaged forests (Scott et al., 2012). Thus, an updated assessment of which forested areas are to be currently prioritized for fuel reduction was needed.

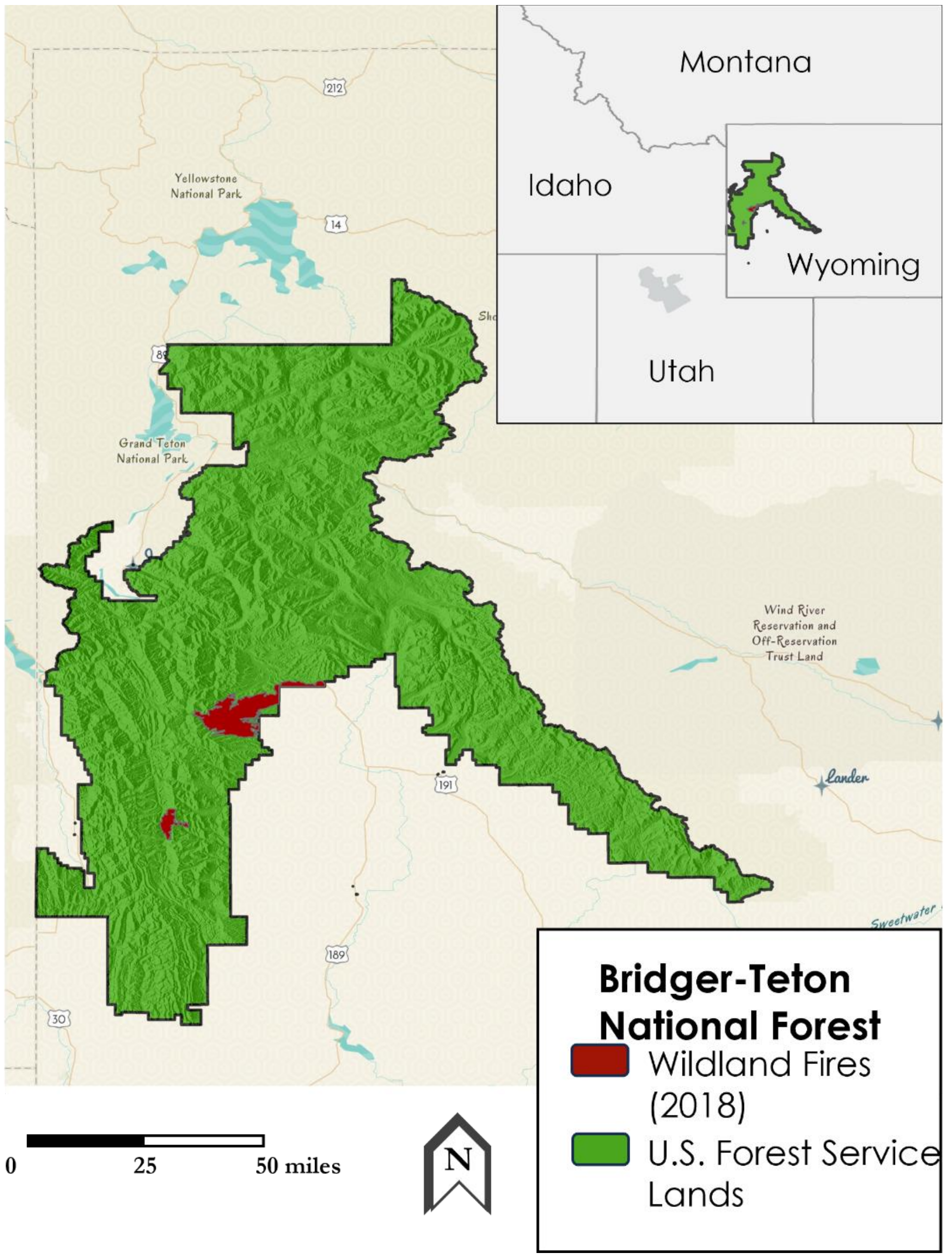

Figure 1. The Bridger-Teton National Forest. Fuel load and fire severity trends for the 2018 wildland fires were analyzed to predict fuel load and fire severity trends in 2023.

2.2 Project Partner & Objectives

We partnered with the USFS Remote Sensing Manager in USFS Region 4 to identify the greatest at-risk areas to wildfire within the BTNF. This project aligns with the USFS's goals of mitigating fire risk for communities and fostering fire-resistant forests. The USFS traditionally employs prescribed burning and forest thinning at various scales, particularly near WUIs, to reduce fuel loads. In one study led by the USFS, thinning within 12 sites led to overall tree density decrease by greater than 60%, reducing susceptibility to crown fires (Harrod, 2009). Through this collaboration, we identified at-risk WUI zones for fuel reduction efforts to inform the USFS's forest management decision-making. Our project completed the following three objectives: 1) map areas with potential for high-severity fires and high fuel loading, 2) inform the partner of current wildfire risk by delineating areas that should be prioritized for fuel reduction to address community safety and 3) create a tutorial document that showcases project methodology to replicate project methods to other wildfire crisis strategy sites that the partner would like to address.

3. Methodology

3.1 Data Acquisition

We acquired all satellite data from the USGS Landsat 8 Operational Land Imager (OLI) Collection 2 Tier 1 Level 2 and NASA Shuttle Radar Topography Mission (SRTM) sensors at the 30 m resolution due to the availability of this spatial resolution (Table 1). Because a greater proportion of BTNF burned in 2018 relative to other years in the past 10 years, we collected imagery across three temporal periods to analyze fuel and fire severity trends from 2017-2019 and predict fuel and fire severity trends in 2023 for random forest models (Table 2).

Table 1
Remote sensing variables

Data Category	Data Product	Variable	Time Period
Spectral Band Indices	Landsat 8 OLI Collection 2 Tier 116-Day 30 m	Normalized Difference Vegetation Index, Normalized Difference Moisture Index, and differenced Normalized Burn Ratio	Pre-Fire, Post-Fire, and Current
Tasseled Cap Indices	Landsat 8 OLI Collection 2 Tier 1 Top of Atmosphere 16-Day 30 m	Brightness, Wetness, Greenness	Pre-Fire, Post-Fire, and Current
Topography	NASA SRTM 11-Day 30 m	Elevation, Slope, Aspect	Derived from SRTM 2007

Table 2
Temporal periods for data acquisition in regards to overall study period for the project

Time Period	Dates	Rationale
Pre-fire in study period	June 1 - October 31, 2017 and June 1 – July 31, 2018	Used to train our random forest models.
Post-fire in study period	August 1 - October 31, 2018 and June 1 - October 31, 2019	Used to calculate the differenced normalized burn ratio.
Current in study period	June 1 - October 31, 2023	Used to predict current fuel load and current fire severity conditions for random forest models.

3.1.1 Ancillary Datasets

We used four ancillary datasets for this project (Table 3). We downloaded a vegetation cover dataset specific to the USFS Intermountain West Region 4 called the Vegetation Classification, Mapping, and Quantitative Inventory (VCMQ; Nelson et al., 2015). VCMQ provided estimates for both shrub and tree canopy cover, ranging from 0-100%. Additionally, we used VCMQ tree size class data that was grouped as non-forested, size class 2 (<5" diameter breast height), size class 3 (5-9.9" diameter breast height), size class 4 (10-19.9" diameter breast height), size class 5 (20-29.9" diameter breast height), and size class 6 (30+" diameter breast height). The second ancillary dataset was LANDFIRE, where we obtained canopy height (m) for aboveground vegetation. Canopy height was categorized as non-forest, low canopy (0-10m), medium canopy (10-25m), and tall canopy (25-50m) (LANDFIRE, 2016). We downloaded both the National USFS Final Fire Perimeters dataset and WUIs from the USDA Forest Service Geodata Clearinghouse (United States

Geological Survey et al., 2021). We used the fire perimeter dataset to identify all fires that occurred in 2018. The WUI highlighted developed areas close to wildland vegetation and at high fire risk as of 2020.

Table 3
Data products

Data Product	**Variable**	**Spatial Resolution**	**Time Period**
Vegetation Classification, Mapping, and Quantitative Inventory (VCMQ)	Canopy Cover (%), Tree Size Classes (Diameter at Breast Height)	30 m	Derived 2014
LANDFIRE	Canopy Height (m)	30 m	Derived 2014
Wildland Urban Interface	Area of Developed Areas that Overlap with Wildland Vegetation	N/A	Derived 2020
National USFS Final Fire Perimeter	Perimeters of Fires that were 10 Acres or Greater in Size	N/A	2018

3.2 Data Processing
To build our random forest models and create our predicted raster datasets for fuel load and burn severity, we first needed to process satellite data and create the variables that would be included in the models. We processed image rasters downloaded directly as image collections in Google Earth Engine (Gorelick et al., 2017). We filtered and clipped images to study area shape files as well as filtered by the pre-fire, post-fire, and current temporal ranges. We used functions and formulas to calculate vegetation indices, Tasseled Cap transformations, and topographic variables through Google Earth Engine, as further explained below. After creating these variables, we exported the images as rasters to be imported by other programs such as ArcGIS Pro 3.2.1.

3.2.1 Vegetation Indices
We processed vegetation indices across specific temporal ranges categorized as pre-fire and post-fire. For the pre-fire period, we selected the time frames of June 1 to October 31, 2017 and June 1 to October 31, 2018. The post-fire periods chosen were August 1 to October 31, 2018, and June 1 to October 31, 2019. These temporal selections were limited to the months of June to October since they best align with when the fire season occurs.

We calculated a total of three vegetation indices. First, the Normalized Difference Vegetation Index (NDVI) indicates the density and health of vegetation where lower values could indicate higher fuel loads, given more dead plant material that could burn (Rouse et al., 1974). Second, the Normalized Difference Moisture Index (NDMI) indicates moisture content where lower values represent drier conditions and therefore more likelihood of areas to burn (Wilson and Sader, 2022). Finally, the difference normalized burn ratio (dNBR) is the difference between normalized burn ratio values from pre-fire to post-fire where higher values indicate a higher burn severity (Parks et al., 2018; Key et al., 2006). The equations for how we calculated each variable are listed below (Equations 1 – 4) where NIR corresponds to the near infrared band, SWIR1 and SWIR2 correspond to the short-wave infrared band 1 and 2 respectively, and RED corresponds to the red band.

$$NDVI = (NIR - RED) / (NIR + RED) \quad \text{Eq. 1}$$

$$NDMI = (NIR - SWIR1) / (NIR + SWIR1) \quad \text{Eq. 2}$$

$$dNBR = (\text{pre-fire } NBR) - (\text{post-fire } NBR) \quad \text{Eq. 3}$$

where NBR = (NIR – SWIR2) / (NIR + SWIR2) Eq. 4

3.2.2 Tasseled Cap Indices

To be able to differentiate soil from vegetation, vegetation from water, and soil from water, we calculated three Tasseled Cap Indices. These indices include brightness, greenness, and wetness and represent information about soil, vegetation, and moisture content, respectively. We first extracted Landsat images from the USGS Landsat 8 Collection 2 Tier 1 top-of-atmosphere (TOA) across the same temporal periods as we did for the vegetation indices. Because the coefficients used in the Tasseled Cap transformation are specific to the spectral characteristics of the satellite imagery being processed, we used a series of mathematical operations and coefficients as determined by Baig and others (2014, page 429) to derive these new spectral indices. Below are the coefficients used to derive the tasseled cap indices (Table 4). The coefficients of each band were added across all bands, with the sum of the bands equaling the new index.

Table 4

Tasseled cap indices

Landsat 8 TOA	Band 2 (Blue)	Band 3 (Green)	Band 4 (Red)	Band 5 (NIR)	Band 6 (SWIR1)	Band 7 (SWIR2)
Brightness	0.3029	0.2786	0.4733	0.5599	0.508	0.1872
Greenness	-0.29412	-0.243	-0.5424	0.7276	0.0713	-0.1608
Wetness	0.1511	0.1973	0.3283	0.3407	-0.7117	-0.4559

3.2.3 Topographic Variables

To create our topographic variables for the Bridger-Teton National Forest, we first obtained a 30-meter Digital Elevational Model (DEM) from NASA SRTM in Google Earth Engine. The DEM provided us with an elevation layer for our study area. Using the terrain function, we then processed the DEM to create an aspect and slope layer (Farr et al., 2007).

3.2.4 Fuel Load and Burn Severity

We used a combination of different categories of canopy height, canopy cover, and tree size class data to determine fuel load levels across the BTNF. We first created a new fuel load field within the attribute table for each vegetation metric (canopy cover, canopy height, and tree size class). We used the select by attributes tool to populate the fuel load field using the categories specified below in ArcGIS Pro (Table 5). Then, we used the merge tool to spatially join all three vegetation layers and create a final fuel load layer that identified low, medium, and high fuel load areas in accordance with all three vegetation variables. We discarded any mismatches in fuel load characterization across the three vegetation variables. For burn severity, we categorized dNBR values into five burn severity categories (Table 6), using methods described by Rozario et al., (2018).

Table 5

Categorization of fuel load levels

Fuel Load	**Canopy Cover (%)**	**Canopy Height (Meters)**	**Tree Size Class (Diameter at Breast Height)**
Low	No canopy cover Shrub: 10-24 Tree: 10-20	Non-forest	Non-forest
Medium	Tree: 20-50	25 - 50	20-29.9” 30” +
High	Shrub: 25-100 Tree: 50-100	0 - 10 10 - 25	<5” 5-9.9” 10-19.9”

Table 6

Categorization of burn severity levels

Severity Level	dNBR Range
Enhanced Growth	< -0.1
Unburned	-0.1 to +0.1
Low Severity	+0.1 to +0.27
Moderate Severity	+0.27 to +0.66
High Severity	> +0.66

3.3 Data Analysis

We computed two supervised classifications with a machine learning random forest model in RStudio (ver. 4.3.2) using the "randomForest" package (Liaw & Wiener, 2002). We designed these random forest models to predict fuel load and burn severity separately based on the 2018 fires. For both random forest models, we chose the following predictor variables from remotely sensed climatic and topographic metrics described above: elevation (m), slope (degrees), aspect (degrees), NDVI, NDMI, brightness, greenness, and wetness. These predictor variables were chosen based on literature review of which variables most affect fire behavior (Hoffrén et al., 2023; Myroniuk et al., 2023). However, we did not look into correlation among predictor variables. Our response variable for the fuel load random forest model was fuel load, which was determined by estimates of canopy cover (%), canopy height (m), and tree size (m) as described above. Our response variable for the fire severity random forest model was dNBR.

We utilized 30% of our observation data to train each random forest model where the remaining 70% of data was used to validate each model with a standardized seed set of 123 samples and 500 simulations to ensure that all possible combinations of different predictor variables were used in assessing which variable combination best predicted the response variable. We chose the final model based on the variables that optimized the random forest model predictive power using the R package "raster" (Hijmans & van Etten, 2012).

4. Results & Discussion

From the final models, we created a predicted fuel load and predicted burn severity raster layer (Figure 2) using 2023 predictor variables. From the predicted fuel load and burn severity raster layers, we overlayed known WUI areas (Figures 3 and 4). These overlapping high burn severity and moderate fuel load areas have been highlighted (Figure 5) as areas to prioritize fuel reduction as they pose the greatest fire risk to communities.

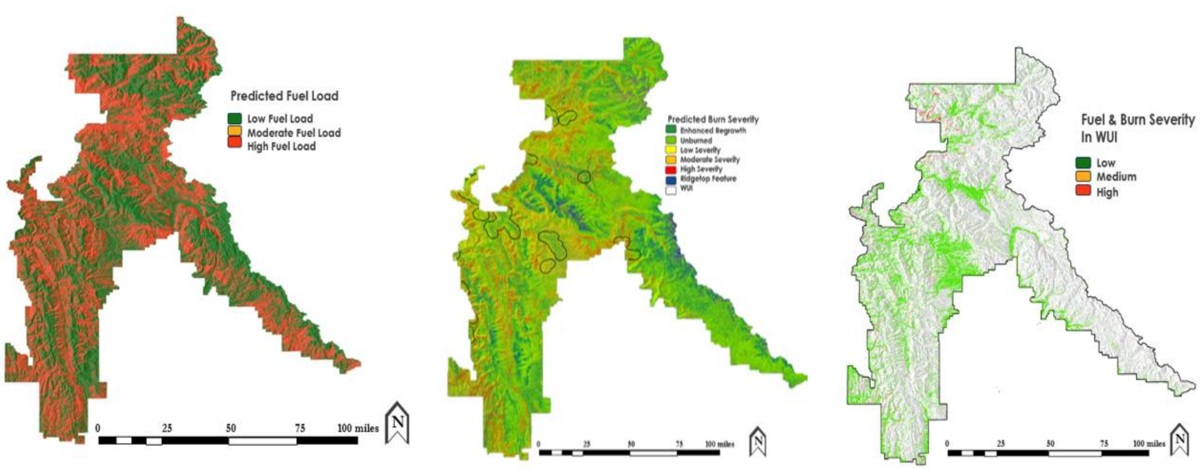

Figure 2. Predicted fuel load (left), burn severity (center), and overlay of both fuel load and burn severity (right) in the Bridger-Teton National Forest.

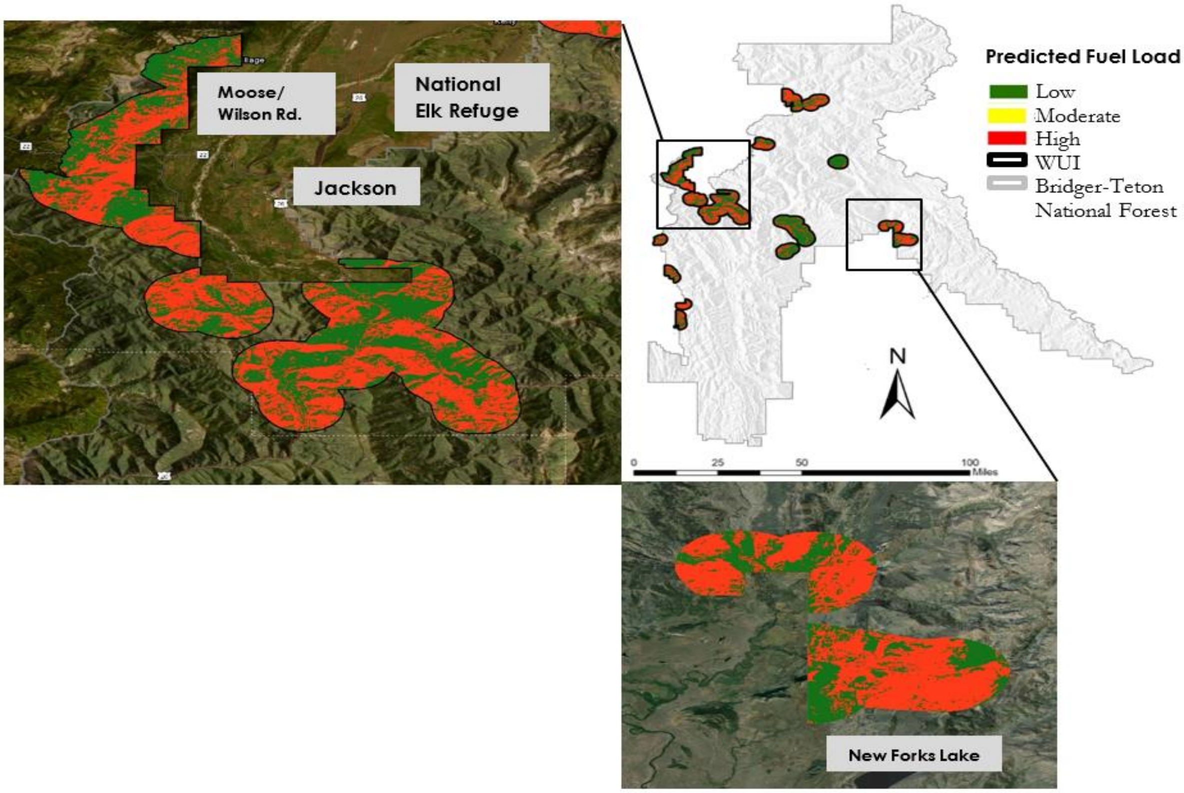

Figure 3. Predicted fuel loads in WUIs near Jackson, Wyoming and New Forks Lake (Cora, Wyoming).

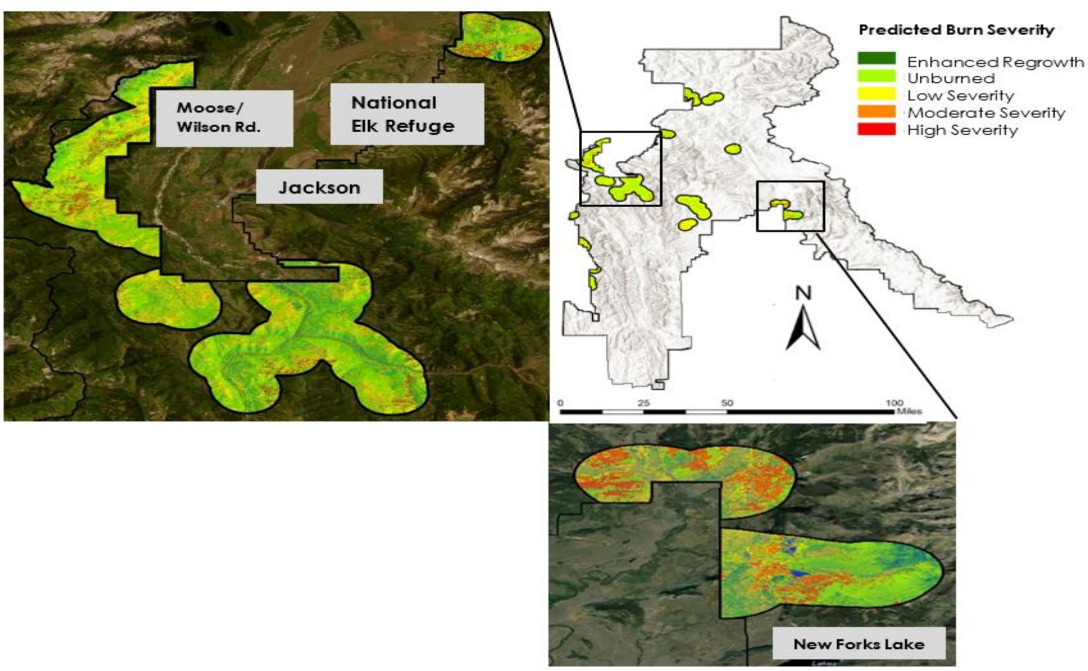

Figure 4. Predicted burn severity in WUIs near Jackson, Wyoming and New Forks Lake (Cora, Wyoming).

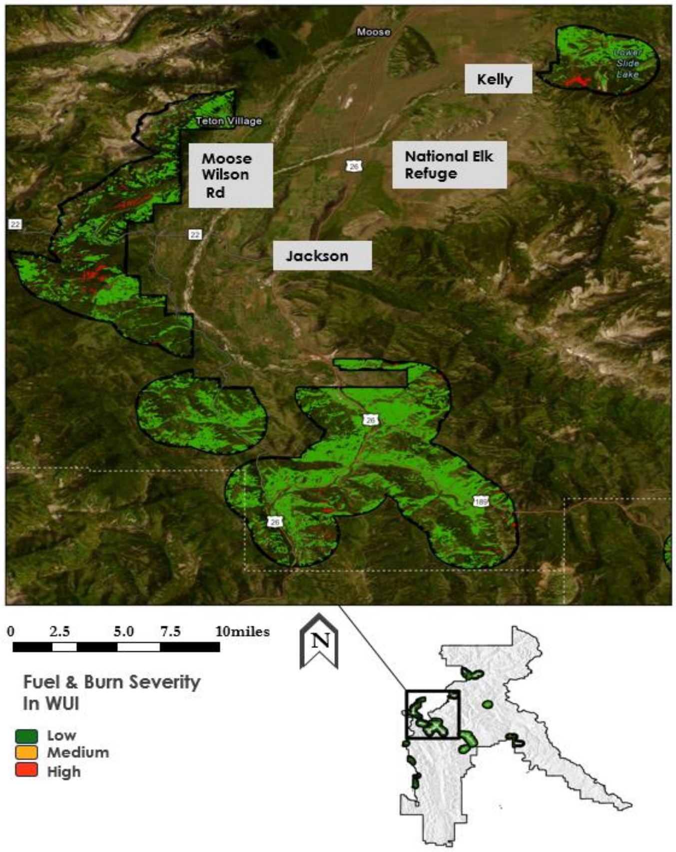

Figure 5. Predicted burn severity and fuel loads in WUI near Jackson, Wyoming within the Bridger-Teton National Forest.

4.1 Analysis of Results

The following predictors: elevation (m), NDVI, Brightness, Wetness, Greenness had the highest predictive power in the fuel load random forest model, where elevation (m), aspect (degrees), and Brightness drove the burn severity model predictive power. We calculated an error rate for the fuel load random forest model, where 12% of low fuel was misclassified as high fuel and 7% of high fuels were misclassified as low fuels (Table 7). In the burn severity model, we calculated classification error, which averaged >50% for unburned, low, and moderate burn severity, meaning that over 50% of the data was misclassified or placed in the incorrect category (Table 8).

Our random forest models trained on random point data within our study area and could not be validated with field data. We anticipate that with field data, fuel load could be re-classified to be more accurate within fine to coarse fuels in current field conditions that could therefore improve model predictive power. Additionally, as we utilized top of atmosphere passive remote sensing tools, our models relied heavily on canopy fuels and coarser dead and live fuel classes, as determined by diameter at breast height tree bole diameters of > 30cm. With a lack of understory remote detection, medium to fine fuels from grasses, herbaceous vegetation, shrubs, pine needles, duff, etc. were under-represented in our models while coarse fuels were possibly over-represented. Though, it is difficult to determine understory fuels as indicated throughout the scientific literature (Saatchi et al., 2007; D'Este et al., 2021). Fuel load is indicative of live and dead vegetation that greatly impacts fire behavior in forested systems as well as throughout WUI. With the lack of model fit in the burn severity and fuel load models, it is difficult to validate predictive fire behavior and community risks in this study. However, it is feasible for these models to be improved and to be utilized as viable tools for future management decisions and community risk assessments.

Table 7

Confusion matrix for predicted fuel load

Predicted Fuel Load	Low	Medium	High	Class Error
Low	96	0	13	0.119
Medium	0	0	0	N/A
High	5	0	63	0.074

Table 8

Confusion matrix for predicted burn severity

	Enhanced Regrowth	Unburned	Low Severity	Moderate Severity	High Severity	Class Error
Enhanced Regrowth	0	0	1	0	0	1.00
Unburned	0	15	12	8	0	0.571
Low Severity	0	12	14	5	0	0.548
Moderate Severity	0	5	5	11	1	0.500
High Severity	0	0	0	1	0	1.00

After overlaying the predicted fuel map and predicted burn severity maps, we calculated acres of forested areas within the WUI to inform the U.S. Forest Service of total areas of each fuel (Table 9) and burn severity category (Table 10). As identified by the fuel load and burn severity within the WUI boundaries (Table 11), there is approximately 74,376 acres that have both low fuels and low burn severity. This is roughly 39% of the total area within the WUI. In contrast, the medium and high area for both fuel load and severity are around 1% of the total area within the WUI. Therefore, when looking at areas that have both high fuel loads and potential for high severity fires, a relatively small proportion of the WUI (1%) needs to be immediately addressed via fuel reduction and should consider employing fireproofing practices. However, considering project limitations as discussed further below, our project likely underestimated total forested areas with high fuel load and high burn severity.

Table 9

Acreage of fuel load in the WUI

Fuel Load	Low	Medium	High
Acres in WUI & % of Area	95302 (50%)	<1 (1%)	95413 (50%)

Table 10

Acreage of burn severity categories in the WUI

Burn Severity Category	Enhanced Regrowth	Unburned	Low Severity	Medium Severity	High Severity
Acres in WUI & % of Area	23 (<1%)	26823 (14%)	103163 (54%)	59695 (31%)	1014 (1%)

Table 11

Acreage of burn severity and fuel load categories combined in the WUI

Fuel & Burn Severity Category	Low Fuel & Low Burn	Medium Fuel & Medium Burn	High Fuel & High Burn

Acres in WUI & % of Area	74376 (39%)	<1 (<1%)	998 (1%)

4.2 Feasibility for Partner Use

We encountered several limitations during this project. Our fuel and burn maps used decade-old data and thus held less than desired current information. Also, our models were based on less relevant vegetation metrics. We were unable to access field data to "ground-truth" our models and verify field conditions. Additionally, we did not find it feasible to utilize ISS GEDI data for the temporal range of this study. Our project found that the partner could utilize several of the methods we employed, and to consider additional tools alongside our methodology to create high accuracy predictive models if these challenges are remedied in the future.

For example, we manipulated and processed preliminary GEDI data and found that when temporal resolution is broad, data coverage is sufficient in the study area. While narrow temporal ranges limit point data and coverage, it is feasible to utilize high-resolution GEDI data when temporal ranges focus on data from December 2018 onward. As it is likely that wildfires will occur in the future, pairing GEDI with vegetation indices and topographic data to investigate landscape conditions prior to, during, and following wildland fire could be substantially more predictive of fuel loads and burn severity (Myroniuk et al., 2023). It would be beneficial to inventory in part and validate field conditions to better simulate and predict fuel classes that validate decision tree methods like random forest models, as this has been a common strategy in other Intermountain West wildland fire studies (Shendryk, 2022).

4.3 Future Recommendations

To better integrate our methods into our partner's future projects, we recommend taking advantage of the finer spatial resolution of GEDI (25 m) as compared to Landsat's resolution (30 m). While we had a time constraint of when GEDI became active, future studies can also take full advantage of extracting canopy cover, terrain elevation, and relative tree height metrics from GEDI for both fine and large fuel loads (Lang et al., 2022). Additionally, our partner could investigate vegetation indices as well which when used in conjunction with GEDI, we think would result in higher power models than we generated in this study.

5. Conclusions

We identified 998 acres that have high fuel loading areas and potential for high-severity fires within the WUI based on our random forest analysis. As the WUI is expected to expand further into Bridger-Teton National Forest, we recommended that forested areas closer to populated areas are prioritized for fuel reduction to address community concerns. These areas include Jackson, Kelly, Moran, New Forks Lake, and Star Valley Ranch. Fuel reduction activities can consist of prescribed burning or mechanical thinning. For areas outside the WUI but still highlighted with high fuel and potential for high severity fires, we recommend less pressing management activities such as timber harvests when resources are available. Finally, with our tutorial document, our partner can now use the same methodology to repeat this project in other national forests prone to wildfires.

When considering the feasibility of this study, there were several limitations. Firstly, with no field data to validate our random forest and verify our fuel loads, the accuracy of our models is not high. This also led to there being a low representation of medium fuel loads for the model to be trained on. As a result, our random forest model is not able to correctly identify medium fuel loads and instead categorized fuel loads either low or high. Another limitation to our datasets is incorporating surface fuels, which can strongly determine fire behavior and patterns. As GEDI was not available until 2019 and our analysis focused on 2018 fires, we recommend future projects leverage remote sensing data like from GEDI to capture vital vegetation characteristics, including canopy height and biomass density, enhancing the accuracy of fuel load assessments. Furthermore, using continuous vegetation metrics data instead of binned datasets for canopy cover, height, and tree size class would likely yield more precise results.

6. Acknowledgements

Our team would like to thank several individuals who made our time with DEVELOP and working on this project enjoyable and overall supported our success. First, thank you to our science advisors Dr. Di Yang and Dr. Austin Madson at the University of Wyoming for their support and guidance as we dove headfirst into the world of GIS. We want to thank our project partner Jed Gregory for the opportunity to give back to the scientific community and Dr. Kenton Ross and Dr. Xia Cai from NASA DEVELOP for meeting with us to provide additional assistance. Finally, we want to thank our NASA DEVELOP Lead Truman Anarella and our NASA DEVELOP Project Coordination Fellow Marisa Smedsrud for providing us with helpful direction when creating our deliverables during our time with DEVELOP.

Any opinions, findings, and conclusions or recommendations expressed in this material are those of the author(s) and do not necessarily reflect the views of the National Aeronautics and Space Administration.

This material is based upon work supported by NASA through contract 80LARC23FA024.

7. Glossary

Diameter at Breast Height – the standard method for measuring the diameter of a standing tree trunk at approximately 1.3m above ground-level
Differenced Normalized Burn Ratio (**dNBR**) – The difference between pre-fire and post-fire burn severity that indicated high damage areas by fires. The normalized burn ratio is calculated with the near-infrared and shortwave-infrared bands.
Earth Observations – Satellites and sensors that collect information about the Earth's physical, chemical, and biological systems over space and time
Fire Behavior – how a fire acts on the landscape as impacted by weather, wind, long-term climate, and fuel loads leading to release of energy (intensity) and vegetation damage and/or mortality
Fuel Load – the combustible material in an area e.g. pine needles, standing dead trees, logs, snags, homes, etc.
Google Earth Engine – is a cloud-based data pipeline service that provides direct access to satellite imagery and geospatial datasets while also providing direct coding interface
Intermountain West – a geographic region in the United States located between the Rocky Mountains in the East and the Cascade and Sierra Nevada Mountains in the West
Landsat 8 Operational Land Imager (**OLI**) and **Top-Of-Atmosphere** (**TOA**) **Sensors** – the OLI sensor was launched in April 2013 and is a type of "push-broom" scanner that takes images of Earth's surface and measures radiation from several spectral bands such as ocean aerosols, blue, green, and near infrared bands at a 15m to 30m resolution. The TOA sensor is a part of the OLI sensor which collects additional spectral bands
Normalized Difference Moisture Index (**NDMI**) – a metric used to detect the moisture within vegetation from the near-infrared and short-wave infrared bands
Normalized Difference Vegetation Index (**NDVI**) – a metric used to detect vegetation photosynthesis and therefore vegetation health and density from the red and near-infrared bands
R Studio (**R**) – open-source integrated development environment (IDE) for the programming language, R for statistical analysis and graphical interpretation
Random Forest – a supervised machine learning technique that operates by constructing decision trees based on training and validation data for separating or grouping data variables for further model classification
Shuttle Radar Topography Mission (**SRTM**) – and international satellite mission that obtained high-resolution digital elevation models (Earth surface elevation) from an eleven-day mission in 2000
Spatial Resolution – the pixel size or the smallest object that can be resolved by a remote sensor or imaging device
Tasseled Cap Transformation – the transformation of spatial information from satellite data into three distinct spectral indicators: brightness, greenness, and wetness
Topography – the surface features of Earth's surface, including elevation, aspect, and slope

Vegetation Classification, Mapping, and Quantitative Inventory (**VCMQ**) – US Forest Service Project through Region 4 to inventory and map shrub cover, tree cover, and vegetation health assessments from 12 Intermountain Region Forests, including the Bridger-Teton National Forest

Wildland Urban Interface (**WUI**) – the line, area, or zone where structures and other human development meet or intermingle with undeveloped wildland or vegetative fuels (Department of Agriculture & Department of Interior 2001).

8. References

Baig, M. H. A., Zhang, L., Shuai, T., & Tong, Q. (2014). Derivation of a tasselled cap transformation based on Landsat 8 at-satellite reflectance. Remote Sensing Letters, 5(5), 423–431. https://doi.org/10.1080/2150704X.2014.915434

Clark-Wolf, K., Higuera, P. E., Shuman, B. N., & McLauchlan, K. K. (2023). Wildfire activity in northern Rocky Mountain subalpine forests still within millennial-scale range of variability. *Environmental Research Letters, 18*(9). https://doi.org/10.1088/1748-9326/acee16

Deeming, J. E., Lancaster, J. W., Fosberg, M.A., Furman, R.W., & Schroeder, M. J. (1972). *National fire-danger rating system*. Rocky Mountain Forest and Range Experiment Station, Forest Service, US Department of Agriculture. https://doi.org/10.5962/bhl.title.98707

Department of Agriculture & Department of Interior. (2001). *Urban wildland interface communities within the vicinity of federal lands that are at high risk from wildfire*. https://www.federalregister.gov/d/01-52

D'Este, M., Elia, M., Giannico, V., Spano, G., Lafortezza, R., & Sanesi, G. (2021). Machine Learning Techniques for Fine Dead Fuel Load Estimation Using Multi-Source Remote Sensing Data. *Remote Sensing*, *13*(9), 1658. https://doi.org/10.3390/rs13091658

Farr, T.G., Rosen, P.A., Caro, E., Crippen, R., Duren, R., Hensley, S., Kobrick, M., Paller, M., Rodriguez, E., Roth, L., Seal, D., Shaffer, S., Shimada, J., Umland, J., Werner, M., Oskin, M., Burbank, D., & Alsdorf, D.E. (2007) The Shuttle Radar Topography Mission. *Reviews of Geophysics*, *45*(2). https://doi.org/10.1029/2005RG000183

Furniss, T. J., Kane, V. R., Larson, A. J., & Lutz, J. A. (2020). Detecting tree mortality with Landsat-derived spectral indices: Improving ecological accuracy by examining uncertainty. *Remote Sensing of Environment*, *237*, 111497. https://doi.org/10.1016/j.rse.2019.111497

Gao, B. C. (1996). NDWI—A normalized difference water index for remote sensing of vegetation liquid water from space. *Remote Sensing of Environment*, 58(3), 257-266. https://doi.org/10.1016/S0034-4257(96)00067-3

Gorelick, N., Hancher, M., Dixon, M., Ilyushchenko, S., Thau, D., & Moore, R. (2017). Google Earth Engine: Planetary-scale geospatial analysis for everyone. *Remote Sensing of Environment, 202*, 18-27. https://doi.org/10.1016/j.rse.2017.06.031

Harrod, R. J. Peterson, D. W., Povak, N. A., & Dodson, E. K. (2009). Thinning and prescribed fire effects on overstory tree and snag structure in dry coniferous forests of the interior Pacific Northwest. *Forest Ecology and Management*, *258*(5), 712-721. https://doi.org/10.1016/j.foreco.2009.05.011

Hijmans, R. J. & van Etten, J. (2012). raster: Geographic analysis and modeling with raster data. R package version 2.0-12. http://CRAN.R-project.org/package=raster

Hoffrén, R., Lamelas, M. T., de la Riva, J., Domingo, D., Montealegre, A. L., García-Martín, A., & Revilla, S. (2023). Assessing GEDI-NASA system for forest fuels classification using machine learning techniques. *International Journal of Applied Earth Observation and Geoinformation*, *116*, 103175. https://doi.org/10.1016/j.jag.2022.103175

Key, C., & Benson, N. (2006). Landscape assessment: Ground measure of severity, the Composite Burn Index; and remote sensing of severity, the Normalized Burn Ratio. In FIREMON: Fire Effects Monitoring and Inventory System (LA 1, pp. 1-51). https://www.researchgate.net/publication/241687027

LANDFIRE 2.0.0. (2016). U.S. Department of Agriculture, Forest Service, U.S. Department of Interior. https://landfire.gov/lf_remap.php

Lang, N., Kalischek, N., Armston, J., Schindler, K., Dubayah, R., & Wegner, J. D. (2022). Global canopy height regression and uncertainty estimation from GEDI LIDAR waveforms with deep ensembles. *Remote Sensing of Environment*, *268*, 112760. https://doi.org/10.1016/j.rse.2021.112760

Liaw, A. & Wiener, M. (2002). Classification and Regression by RandomForest. *Forest*, *23*. https://www.researchgate.net/publication/228451484_Classification_and_Regression_by_RandomForest

Miller, C., & Urban, D. (2000). Connectivity of forest fuels and surface fire regimes. *Landscape Ecology*, *15*, 145-154. https://doi.org/10.1023/A:1008181313360

Morton, D. C., Roessing, M. E., Camp, A. E., & Tyrrell, M. L. (2003). Assessing the environmental, social, and economic impacts of wildfire [GISF Research Paper 001]. Yale University. https://yff.yale.edu/sites/default/files/files/wildfire_report(1).pdf

Myroniuk, V., Zibtsev, S., Bogomolov, V., Goldammer, J. G., Soshenskyi, O., Levchenko, V., & Matsala, M. (2023). Combining Landsat time series and GEDI data for improved characterization of fuel types and canopy metrics in wildfire simulation. *Journal of Environmental Management*, *345*, 118736. https://doi.org/10.1016/j.jenvman.2023.118736

Nelson, M. L., Brewer, C. K., & Solem, S. J. (2015). *Existing vegetation classification, mapping, and inventory technical guide version 2.0* (Gen. Tech. Rep. WO–90). U.S. Department of Agriculture, Forest Service, Ecosystem Management Coordination Staff. https://www.fs.usda.gov/emc/rig/documents/protocols/vegClassMapInv/EVTG_v2-0_June2015.pdf

Parks, S., Holsinger, L., Voss, M., Loehman, R., & Robinson, N. (2018). Mean Composite Fire Severity Metrics Computed with Google Earth Engine Offer Improved Accuracy and Expanded Mapping Potential. *Remote Sensing*, *10*(6), 879. https://doi.org/10.3390/rs10060879

Radeloff, V. C., Hammer, R. B., Stewart, S. I., Fried, J. S., Holcomb, S. S., & McKeefry, J. F. (2005). THE WILDLAND–URBAN INTERFACE IN THE UNITED STATES. *Ecological Applications*, *15*(3), 799–805. https://doi.org/10.1890/04-1413

Radeloff, V. C., Mockrin, M. H., Helmers, D., Carlson, A., Hawbaker, T. J., Martinuzzi, S., Schug, F., Alexandre, P. M., Kramer, H. A., & Pidgeon, A. M. (2023). Rising wildfire risk to houses in the United States, especially in grasslands and shrublands. *Science*, *382*(6671), 702–707. https://doi.org/10.1126/science.ade9223

Rouse, J. W., Haas, R. H., Schell, J. A., & Deering, D. W. (1974). Monitoring vegetation systems in the Great Plains with ERTS. *Proceedings of the Third Earth Resources Technology Satellite-1 Symposium*, 1, 309-317. https://ntrs.nasa.gov/api/citations/19740022614/downloads/19740022614.pdf

Rozario, P., Madurapperuma, B., & Wang, Y. (2018). Remote Sensing Approach to Detect Burn Severity Risk Zones in Palo Verde National Park, Costa Rica. *Remote Sensing*, *10*(9), 1427. https://doi.org/10.3390/rs10091427

Saatchi, S., Halligan, K., Despain, D. G., & Crabtree, R. L. (2007). Estimation of Forest Fuel Load From Radar Remote Sensing. *IEEE Transactions on Geoscience and Remote Sensing*, *45*(6), 1726–1740. https://doi.org/10.1109/TGRS.2006.887002

Scott, J. H., Helmbrecht, D. J., Parks, S. A., & Miller, C. (2012). Quantifying the threat of unsuppressed wildfires reaching the adjacent wildland-urban interface on the Bridger-Teton National Forest, Wyoming, USA. *Fire Ecology*, *8*, 125-142. https://doi.org/10.4996/fireecology.0802125

Scott, J. H., Thompson, M. P., & Calkin, D. E. (2013). *A wildfire risk assessment framework for land and resource management.* US Department of Agriculture, Forest Service, Rocky Mountain Research Station. http://dx.doi.org/10.2737/rmrs-gtr-315

Shendryk, Y. (2022). Fusing GEDI with earth observation data for large area aboveground biomass mapping. *International Journal of Applied Earth Observation and Geoinformation*, *115*, 103108. https://doi.org/10.1016/j.jag.2022.103108

Shukla, P. R., Skea, J., Slade, R., Al Khourdajie, A., van Diemen, R., McCollum, D., Pathak, M., Some, S., Vyas, P., Fradera, R., Belkacemi, M., Hasija, A., Lisboa, G., Luz, S., & Malley, J. (2022). Climate Change 2022: Mitigation of Climate Change. Contribution of Working Group III to the Sixth Assessment Report of the Intergovernmental Panel on Climate Change. *Cambridge University Press*. https://doi.org/10.1017/9781009157926

Stefanidou, A., Gitas, I. Z., Korhonen, L., Georgopoulos, N., & Stavrakoudis, D. (2020). Multispectral lidar-based estimation of surface fuel load in a dense coniferous forest. *Remote Sensing*, *12*(20), 3333. https://doi.org/10.3390/rs12203333

United States Department of Agriculture. (n.d.). *Welcome!*. Bridger-Teton National Forest. https://www.fs.usda.gov/btnf

United States Geological Survey, United States Department of Agriculture Forest Service, & Nelson, K. (2021). *Monitoring Trends in Burn Severity* (Version 7.0) [Data set]. https://doi.org/10.5066/P9IED7RZ

Wilson, E. H., & Sader, S. A. (2002). Detection of forest harvest type using multiple dates of Landsat TM imagery. Remote Sensing of Environment, 80(3), 385–396. https://doi.org/10.1016/S0034-4257(01)00318-2